Geophysical Research Letters

RESEARCH LETTER
10.1029/2020GL091213

Global Venus-Solar Wind Coupling and Oxygen Ion Escape

M. Persson[1,2], Y. Futaana[1], R. Ramstad[3], A. Schillings[2], K. Masunaga[3], H. Nilsson[1], A. Fedorov[4], and S. Barabash[1]

[1]Swedish Institute of Space Physics, Kiruna, Sweden, [2]Department of Physics, Umeå University, Umeå, Sweden, [3]Laboratory for Atmospheric and Space Physics, University of Colorado, Boulder, CO, USA, [4]Institute of Research in Astrophysics and Planetology UPS, CNRS, Toulouse, France

Key Points:

- The total escaping power from Venus does not increase linearly with increasing available power in the solar wind
- The coupling coefficient, that is, ratio between power out and in, decreases with increasing solar wind energy flux
- The trend of the coupling coefficient with the upstream parameters for Venus is similar to that of Mars but different from that of Earth

Correspondence to:
M. Persson,
moa.persson@irf.se

Citation:
Persson, M., Futaana, Y., Ramstad, R., Schillings, A., Masunaga, K., Nilsson, H., et al. (2021). Global Venus-Solar wind coupling and oxygen ion escape. *Geophysical Research Letters*, *48*, e2020GL091213. https://doi.org/10.1029/2020GL091213

Received 13 OCT 2020
Accepted 16 JAN 2021

Abstract The present-day Venusian atmosphere is dry, yet, in its earlier history a significant amount of water evidently existed. One important water loss process comes from the energy and momentum transfer from the solar wind to the atmospheric particles. Here, we used measurements from the Ion Mass Analyzer onboard Venus Express to derive a relation between the power in the upstream solar wind and the power leaving the atmosphere through oxygen ion escape in the Venusian magnetotail. We find that on average 0.01% of the available power is transferred, and that the percentage decreases as the available energy increases. For Mars the trend is similar, but the efficiency is higher. At Earth, the ion escape does not behave similarly, as the ion escape only increases after a threshold in the available energy is reached. These results indicate that the Venusian induced magnetosphere efficiently screens the atmosphere from the solar wind.

Plain Language Summary Today, there is barely any water on Venus, but presumably a large amount existed in its earlier history. Therefore, the water must have been lost over the course of the Venusian history. An important process for removal of water is escape to space, induced by the interaction between the Venusian atmosphere and the solar wind (a fast stream of particles ejected from the Sun). In this study, we investigated the connection between the energy available in the upstream solar wind and the energy leaving Venus in the form of oxygen ion escape. By characterizing this relation, we investigate how the Venusian atmosphere reacts to changes in the upstream solar wind and how well it protects itself from atmospheric loss caused by the solar wind. We find that the energy transfer decreases as the available upstream energy increases, a trend that is very similar to that found at Mars. However, the Venusian atmosphere seems to absorb less energy from the solar wind than Mars. This indicates that the Venusian induced magnetosphere efficiently screens the atmosphere from the solar wind. This is important for the understanding of the effect of the solar wind on the Venusian atmospheric evolution.

1. Introduction

At present day, the Venusian atmosphere is crushingly dense, and contains almost no water. Yet, measurements indicate that Venus once had a significant amount of water, enough to create a global equivalent water depth of 4–525 m (Way et al., 2016). Therefore, the atmosphere must have evolved over the past few billion years. There are several mechanisms that can affect the planetary evolution, which can be categorized into two main parts: (1) interaction between the atmosphere and the surface and (2) the escape of atmospheric particles to space (Futaana et al., 2017), here we only consider mechanism (2). For ions to escape to space they need to gain enough energy to reach above escape velocity (~10 km/s at Venus). Ions measured in the upper ionosphere of Venus have velocities of ~2–10 km/s (Knudsen et al., 1980; Persson et al., 2019). Therefore, the ions need an additional acceleration to escape. Several processes can potentially provide this additional acceleration, and one of the most important processes is the direct interaction between the solar wind and the Venusian ionosphere. The interplanetary magnetic field, frozen into the solar wind particle flow, induces currents in the Venusian ionosphere. These currents induce a magnetic field that, together with the thermal pressure of the ionospheric particles, is capable of diverting the solar wind flow around Venus (Luhmann et al., 2004). Even though the majority of the solar wind flow is diverted around Venus, the interaction between the solar wind and the Venusian upper atmosphere transfers energy and momentum from the solar wind to the upper atmospheric particles. This energy transfer can provide

the additional energy needed to reach escape energy (~8 eV for O^+). Today, the escape rate of heavy ions from Venus is (3–6)·10^{24} O^+/s (Futaana et al., 2017), and is positively correlated with the solar wind energy flux (Persson et al., 2020a). From the relation between the solar wind energy flux and the O^+ escape rate, Persson et al. (2020a) extrapolated the escape rates back in time to 3.9 Ga. They showed that the total escape from Venus, assuming the same atmospheric conditions and interaction between the solar wind and the atmosphere over the entire period, and that the O^+ comes from water, can explain a global water depth of ~0.02–0.6 m, which is significantly lower than the expected historical 4–525 m (Way et al., 2016).

The energization of the ions depends on how efficient the energy transfer is from the solar wind to the ionospheric ions. The efficiency of the energy transfer may depend on a number of intrinsic and external parameters. Therefore, the efficiency could differ between planets, due to either the differences in their interaction with the solar wind, their difference in atmospheric composition, the difference in the upstream properties of the solar wind and the solar extreme ultraviolet (EUV) flux at their location, or the difference in the area over which the energy can be transferred. For Venus, the area over which energy is transferred from the solar wind to the ionosphere is assumed as the induced magnetosphere boundary (IMB, also known as the ion composition boundary), as this is the boundary over which the solar wind can directly interact with the ionospheric ions (e.g., Lundin et al., 2014; Perez-de-Tejada, 1980).

A coupling efficiency between the Martian escape rate and the solar wind show that ~0.7% of the available solar wind energy is transferred to the atmospheric particles that escape, and that the efficiency decreases both with increased solar wind dynamic pressure and with the EUV flux (Ramstad et al., 2017). At Earth, the ion escape processes are different from those at Venus and Mars due to Earth's intrinsic magnetic field. Ions are accelerated upward from the ionosphere to higher altitudes by heating processes, such as transverse heating (Bouhram et al., 2005; Slapak 2011; Strangeway et al., 2005), field-aligned electric fields (Maggiolo et al., 2006), and centrifugal acceleration (Nilsson et al., 2008, 2012), and creates ion outflow (Kronberg et al., 2014; Moore et al., 2014). The ions that are sufficiently accelerated will reach the plasma mantle, where ~98% of the ions will escape from Earth and the remaining 2% return and re-circulate in the magnetosphere through the plasma sheet (Schillings et al., 2020). An important factor for the escape from Earth is the interplanetary magnetic field (IMF) orientation, where the O^+ transport within the magnetosphere differs between a northward and southward IMF orientation, due to the differences in magnetic topology (Dungey, 1961). The differences cause larger O^+ escape rates for a southward IMF orientation compared to a northward orientation (Cully et al., 2003; Lennartsson et al., 2004; Slapak et al., 2015). In addition, Schillings et al. (2019) showed that the O^+ ion escape through the plasma mantle increases with an increase in the available energy that can enter the system, however, the increase in escape was only present after a threshold in the available energy was reached. Lennartsson et al. (2004) also showed that the average energy of the escaping ions decreases with an increase in the available energy. These differences indicate that the coupling efficiency behaves differently for Earth than for Venus and Mars.

The coupling efficiency and its dependence on upstream parameters tell us how the interaction with the solar wind might change over time, as the upstream parameters changed over the evolution of the Sun (e.g., Ribas et al., 2005; Wood, 2006). In this study, we aim at characterizing how good the energy transfer is from the solar wind to the Venusian ionospheric O^+ ions that escape through the magnetotail, which is the major escape channel for Venus today (e.g., Lammer et al., 2006). Here, we only consider the efficiency of the energy transfer from the solar wind to the ions escaping from the Venusian atmosphere. The total efficiency is dependent on how much energy is transferred to other parts of the Venusian atmosphere, such as to the thermospheric neutral population, or to other ions and neutrals escaping, in addition to the escape of O^+ ions in the Venusian magnetotail. By comparing the available power in the solar wind with the power escaping the planet through O^+ ion escape, we aim at characterizing the coupling efficiency and how it changes with the upstream conditions.

2. Instrumentation and Method

The coupling efficiency of the energy transfer from the solar wind to the Venusian O^+ ion escape is calculated as the ratio between the total power available in the solar wind P_{SW} and the total power escaping from Venus P_Q. The available power in the solar wind is calculated as the energy flux $F_{SW,\,energy}$ times the area

A_{SW} over which the solar wind can transfer its energy to the atmospheric particles. The area is assumed as a disk with the radius of the IMB in the terminator plane of 1.109 R_V (Martinecz et al., 2008; R_V = Venus radii = 6,052 km). The potential dependencies of this area with respect to upstream parameters were investigated, but the dependency was small. According to Martinecz et al. (2008) the solar wind dynamic pressure does not affect the size of the IMB near the terminator. The escaping power is calculated by integrating the energy spectra of the escaping ions $Q_{O^+}(E_m)$ multiplied with the energy E_m. The ratio provides the coupling coefficient

$$k = \frac{P_Q}{P_{SW}} = \frac{\sum_m Q_{O^+}(E_m) \cdot E_m}{F_{SW,E} \cdot A_{SW}}. \quad (1)$$

Here, we calculate the coupling coefficient as a function of upstream parameters in order to see potential variations in the efficiency of the energy transfer from the solar wind to the escaping ions. To calculate the upstream solar wind energy flux and the O^+ ion escape we use data from the Ion Mass Analyzer (IMA), part of the Analyzer of Space Plasma and Energetic Atoms (ASPERA-4) instrument suite (Barabash et al., 2007), on board the Venus Express (VEx) mission (Svedhem et al., 2007). IMA measures ions of energy 0.01–36 keV with an energy resolution of ΔE/E = 7%. The total ~2π field-of-view is differentiated by 16 azimuth sectors with a width of 22.5° each, and elevation deflector plates which sweep 90° in 16 steps with a width of 5.6° each. IMA has moderate mass separation capabilities, using an assembly of permanent magnets that allows for separating ions by their mass-per-charge. Here, we assume that all the measured heavy ions are O^+ (Fedorov et al., 2011). For more details about the instrument see Barabash et al. (2007). To formulate the coupling coefficient and its dependence on the upstream parameters, we use all measurements of IMA obtained from April 2006 to November 2014.

The average O^+ escape rates in the magnetotail are calculated using a method of averaging VEx instantaneous (192 s) distributions into average differential flux distributions, as developed by Persson et al. (2018), and improved by Persson et al. (2020a). Assuming that the plasma environment reacts systematically to the upstream conditions of the Sun and solar wind, the average distributions can be used to calculate the average ion escape rate, and subsequently the coupling coefficient, as a function of the upstream conditions. To find this function, the measurements are binned into 10 groups of upstream parameters (five solar wind energy flux bins and two solar EUV flux bins) in order to calculate the average distributions for each upstream condition.

The average differential flux distributions in the magnetotail are organized by five degrees of freedom: One for the energy of the ions (E), two for the ion flow directions (φ,θ), and two for the spatial position (X, R). The spatial bins are defined from the Venus-Solar-Orbiter (VSO) cylindrical geometric frame, where the X_{VSO}-axis points along the Venus-Sun line, and R_{VSO} is the distance from the X_{VSO}-axis. The spatial bins has a width of $\Delta X = \Delta R = 0.3$ R_V, over the range $X_{VSO} = [-2.3, -1.4]$ R_V and $R_{VSO} = [0, 1.2]$ R_V. For each spatial bin the average 5-dimensional differential flux $\bar{J}(X_i, R_j, \varphi_k, \theta_l, E_m)$ is calculated through an arithmetic mean of all measurements, from each of the 10 groups of upstream parameters, within that spatial bin. The energy is arbitrarily chosen to be divided with ΔE so that it is linearly distributed in velocity space with Δv = 5 km/s. The angular space is divided to have azimuth bin size of $\Delta\varphi = 7.2°$ and elevation bin size of $\Delta\theta = 3.6°$. The energy flux in each bin is calculated from an integration of the average O^+ differential energy flux as

$$F_x(E_m, X_i, R_j) = \sum_{k,l} \bar{J}(X_i, R_j, \varphi_k, \theta_l, E_m) \cos^2(\theta_l) \cos(\varphi_k) \Delta\varphi \Delta\theta \Delta E_m. \quad (2)$$

Note that the flying direction φ,θ, energy E and differential flux $\bar{J}$ are here corrected for the spacecraft velocity. The spacecraft potential is assumed to be insignificant in comparison with the lowest measured ions. Typically, the spacecraft potential varies between ~±5 eV, as found by both modeling (Garrett, 1981) and measurements (Collinson et al., 2016). Therefore, the potential is assumed to not greatly affect the ion measurements (e.g. Bergman et al., 2020). The average escape energy spectra is then calculated through an integration of the energy flux over the disk of the magnetotail, and averaged over the number of slices in the X_{VSO}-direction as

$$Q_{O^+}(E_m) = \frac{1}{N}\sum_i\sum_j F_x(E_m, X_i, R_j)2\pi R_j \Delta R, \quad (3)$$

where N is the number of slices used in the X_{VSO}-direction, R_j is the radius of the center of the spatial bin used, and ΔR is the radial width of the spatial bin. The energy flux is averaged over the slices in the X_{VSO}-direction in order to account for the variations in numbers of measurements (between five and 50) for each spatial location and group of upstream conditions.

The solar EUV flux is estimated using Earth-based measurements, using the Solar EUV Experiment (SEE) on the Thermosphere Ionosphere Mesosphere Energetics Dynamics (TIMED) spacecraft (Woods et al., 2005). The measurements at Earth are propagated to Venus by scaling the intensity and finding the nearest point in time that Venus observed the same solar disk. The estimated error on this propagation is less than ∼7%, due to the quasistable EUV irradiance from the solar disk on timescales of several days (Ramstad et al., 2018; Thiemann et al., 2017). The two EUV flux bins are defined by a division at an average of 7 mWm^{-2}. The upstream solar wind energy flux is calculated from IMA measurements of the H^+ flux distributions outside the bow shock, at the inbound and outbound orbit portion. The valid solar wind H^+ distributions (excluding measurements without full coverage of the solar wind distribution) are used to calculate the solar wind densities and bulk velocities. The measured average solar wind energy flux and propagated solar EUV flux closest to the measurement point is used as the binning parameter for each measurement. Here, we assume that the solar wind properties remain stable between the measurement of the O^+ differential flux and the solar wind moment. On a statistical basis, the error of this assumption is small, as the time between measurements in the solar wind and measurements inside the Venusian induced magnetosphere is less than 2 h due to the highly elliptical orbit of Venus Express, and the error becomes large after ∼10 h (Marquette et al., 2018). The five solar wind energy flux is defined as 0.023–1.8, 1.8–2.7, 2.7–3.8, 3.8–5.9, and 5.9–28 (10^{15} eV m^{-2} s^{-1}). The bin division of the solar EUV flux and solar wind energy flux is the same as deployed in Persson et al. (2020a).

The calculated average escape energy spectra and the available solar wind power is then used to calculate the coupling coefficient as formulated in Equation 1. From the average escape power for each group of upstream parameters we get the total power leaving the Venusian atmosphere in the form of escaping ions, the numerator of Equation 1, and from the upstream parameters we obtain the total power available that can enter the Venusian plasma environment from the solar wind, the denominator of Equation 1.

3. Results and Discussion

The relation between the solar wind power P_{SW} and the escape power P_Q is plotted in Figure 1a, and the coupling coefficient k (Equation 1) as a function of the solar wind energy flux $F_{SW,E}$ in Figure 1b. From Figure 1a it is clear that the escape power in general increases with increasing solar wind power. The relation between the escape rate and the upstream energy flux was already found and discussed in Persson et al. (2020a). Figure 1b shows that even though there is a positive correlation between escape power and available power, the coupling coefficient decreases with increasing solar wind energy flux, as indicated with the simple fitted line to the low EUV cases.

A fitted line to the high EUV cases is less straightforward due to the apparent v-shaped trend. The highest solar wind energy flux case indicates a higher coupling than expected from the general trend. This trend may be explained by the presence of extreme space weather events, such as Interplanetary Coronal Mass Ejections (ICMEs). These events are short bursts of solar plasma that is ejected at high speeds from the Sun and travel through interplanetary space. As they arrive at Venus, they will interact with the Venusian induced magnetosphere and can potentially increase the local escape rates by orders of magnitude (Luhmann et al., 2007). However, it is challenging to measure the global picture of the Venusian plasma environment during transient events, such as ICMEs, with only one spacecraft. The general escape during a transient event can instead be calculated from averaging over many high solar wind energy flux events, to get an average global picture of the effect on the Venusian plasma environment. It was shown that for high dynamic pressure events during solar minimum (approximately corresponding to the low EUV cases used here) in

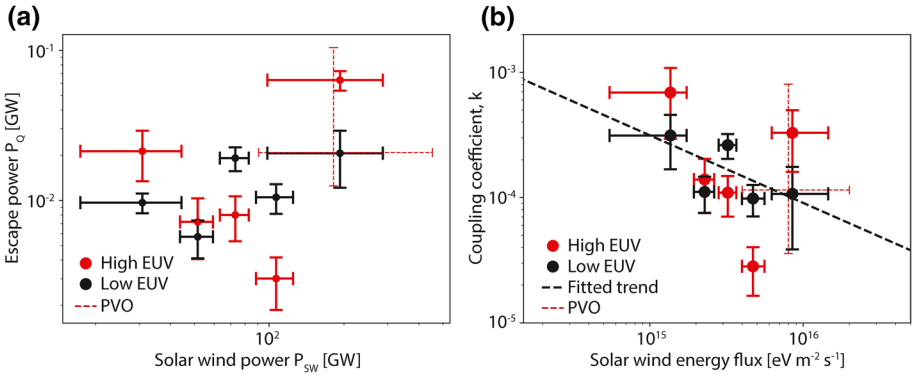

Figure 1. (a) Relation between the power of the escaping particles and the upstream solar wind power. (b) The ratio between the power of the escaping particles and the upstream solar wind power, the coupling coefficient, as a function of the upstream available solar wind energy flux. The red dashed crosses represents the estimated results from the PVO mission, and the black dashed line in (b) is a fitted trend to the low EUV condition. EUV, extreme ultraviolet; PVO, Pioneer Venus Orbiter.

general the escape rates increase by a factor 1.9 (Edberg et al., 2011; Persson et al., 2020a) and by a factor 3.8 for the high EUV cases (approximately corresponding to solar maximum; Persson et al., 2020a). Therefore, as the transient events can drastically increase the escape rates, they will increase the coupling between the upstream solar wind energy and the escape rates. Here, the separation of the upstream condition is made so that there is approximately the same number of measurements in each bin, however, there may still be large variations within the bins, specifically for the lowest and highest solar wind energy flux bins. Therefore, the apparent difference between the high and low EUV flux cases seen in Figure 1b may, at least partly, be explained by that there are generally more extreme solar wind events during solar maximum than during solar minimum (Webb & Howard, 1994).

An estimation of the coupling coefficient found by the measurements from the Pioneer Venus Orbiter (PVO) mission is included in Figure 1. The escape rate ranges from 6×10^{24} O^+/s (McComas et al., 1986) to 5×10^{25} O^+/s (Brace et al., 1987), and the solar wind energy flux range is estimated as 4×10^{15}–2×10^{16} eV m^{-2} s^{-1}, from the measured upstream solar wind density and velocity conditions by PVO (McEnulty, 2012). Using the average escape rate of 1×10^{25} O^+/s and energy of 13 eV, measured in the nightside region by PVO (Brace et al., 1987), the average escaping power is 0.02 GW. This lies in a good agreement with the escaping power of 0.003–0.07 GW found here using VEx measurements (Figure 1). In addition, the approximate coupling coefficient (Equation 1) calculated for the PVO measurements also lies in good agreement with the VEx results. However, it is important to note that the measurements from PVO gave a large range of escape rates, and that the full energy spectra were not measured, which provides large error bars on the escaping power. The measurements from VEx and PVO were also made using different instruments and techniques. Therefore, the PVO estimations added in Figure 1 should be interpreted with care and are not intended to be used to draw large conclusions.

It is important to note that our calculations only include the O^+ ion escape through the magnetotail. By adding other ion or neutral species in the total power leaving the planet, the coupling coefficient will increase. The largest neutral O escape channel is sputtering, which is estimated to be about 25% of the total O^+ ion escape (Lammer et al., 2006), and the O^+ escape is ~30% through the magnetosheath and 70% in the magnetotail (Masunaga et al., 2019). Accounting for the additional escape channels, assuming that the magnetosheath energy spectra is the same as in the magnetotail, and that the average energy of the sputtered O is 10 eV, the average coupling coefficient is increased by a factor between 1.4 and 2.1 for each upstream condition. This increase is marginal, within the error bars of the result in Figure 1b, and does not change the major conclusions of this study. We may also include hydrogen in the results, which is the other major escaping species from Venus. The largest escape channels for hydrogen are ion escape in both the magnetosheath and the magnetotail, and through photochemical reactions (Lammer et al., 2006). The total H escape rate is ~2–4 times larger than the O^+ escape rate (Fedorov et al., 2011; Lammer et al., 2006; Persson

et al., 2020a). The mass of a hydrogen atom is 16 times lower than an oxygen atom, which leads to that the escaping energy from hydrogen is 4–8 times lower than the escaping energy from oxygen. Therefore, the hydrogen component was neglected in the energy budget calculations of this study.

The majority of the energy transfer from the solar wind to the escaping ions is expected to occur near the boundary between the solar wind protons in the magnetosheath and the ionospheric ions in the induced magnetosphere (e.g., Perez-de-Tejada, 1980; Lundin et al., 2014). In this study, we have assumed that the IMB at the terminator represents the energy transfer area, which was shown to not be correlated with the upstream dynamic pressure (Martinecz et al., 2008). As the majority of the energy transfer presumably occurs near the ionosphere, where most of the ions are produced, any potential variabilities of the size of the downstream magnetotail is assumed to not affect the coupling coefficient. The correlation between the IMB and EUV flux is not yet fully determined. However, any dependence on the EUV flux will only affect the absolute value of the coupling coefficient in this study, not the trend of decreasing with an increase in the solar wind energy flux. If the area of energy transfer instead was assumed as the bow shock at the terminator, the available power would increase by approximately a factor of three, and the average coupling coefficient would decrease from 0.01% to 0.003%. The bow shock shape was shown from both VEx and PVO measurements not to be dependent on the solar wind dynamic pressure, but does increase in size with an increase in the solar EUV flux (e.g., Martinecz et al., 2008; Russell et al., 1990; Slavin et al., 1980). Therefore, we conclude that the choice of boundary for energy transfer from the solar wind to the ionospheric ions does not affect the trends over the solar wind energy flux of the coupling coefficient found in this study, only its absolute value.

Even when using a small area such as the terminator plane IMB cross section for the calculation of the total available energy of the upstream solar wind, the coupling is low. Only between 0.003% and 0.07%, with an average of ∼0.01%, of the available solar wind power is transferred to the escaping ions. This indicates that the Venusian plasma environment efficiently screens the ionosphere from the solar wind. The induced magnetosphere is capable of diverting the majority of the amount of incoming energy around itself, rather than channeling it to the ionosphere. Determining the detailed physical processes responsible for the low coupling and its decrease with the increased solar wind energy flux is left for future studies. However, we might speculate that the general decrease in the coupling with the increase in available energy in the solar wind, specifically for low EUV conditions, can be explained by two parts: (i) the energy transfer from the solar wind to the upper atmospheric particles becomes less efficient, and (ii) the energy transferred to the upper atmospheric particles is also deposited to the lower atmosphere through the thermosphere-ionosphere coupling. The deposition of solar wind energy to the lower atmosphere was indicated by a loss of momentum of the solar wind with a decreased altitude in the Venusian exosphere (Lundin et al., 2011, 2014). Further study of the solar wind-ionosphere-thermosphere coupling is needed to include the energy transfer from the solar wind to the thermosphere in the coupling efficiency.

The coupling coefficient between the solar wind and the ion escape from Venus can be compared with both Mars and Earth. The average coupling coefficient at Mars was found to be ∼0.7% (Ramstad et al., 2017), which is a factor ∼100 higher than the average coupling coefficient of 0.01% at Venus. As Venus is larger, the induced magnetosphere, and thus the radius of the interaction area, is almost twice as large. In addition, the solar wind energy flux is higher at Venus, due to the increase in average solar wind density with decreasing distance to the Sun. Therefore, the amount of energy that can potentially be transferred to the escaping ions is larger at Venus, compared to Mars. However, the average escape of atmospheric particles is similar, $\sim 2 \times 10^{24}$ s^{-1} at Mars (Ramstad et al., 2015), compared to $(3–6) \times 10^{24}$ s^{-1} at Venus (Futaana et al., 2017), which means that the Martian escape rates are higher with respect to the potential input of energy to the system compared to Venus. One fundamental difference between Venus and Mars is the size of the planet, and thus their gravity. As the gravity is lower on Mars, the particles do not need as much energy transferred from the solar wind in order to escape the planet. Therefore, Venus gravity presumably acts as a stronger trap for the atmospheric particles. The details of the physical reason for the difference between the two planets is left for future studies.

To compare the coupling coefficient with Earth we need to estimate the average escaping energy. The average O^+ escape rate in the plasma mantle is $(0.3–10) \times 10^{25}$ s^{-1} (Schillings et al., 2019) and the average O^+ temperature near 10 R_E (R_E = Earth's radii = 6,371 km) is 1–2 keV (Nilsson et al., 2013). Thus, the

escaping power is ~1–30 GW, which is one to two orders of magnitude higher than for both Mars (Ramstad et al., 2017) and Venus. The incoming energy at Earth is ~100 GW (Schillings et al., 2019), which gives an average coupling coefficient of around 1%–30%. Therefore, the coupling coefficient at Earth is one to two orders of magnitude higher than for both Venus and Mars, which indicates that more of the available energy is transferred to the escaping ions at Earth. In addition, the coupling trend is expected to behave differently at Earth than for Mars and Venus, due to that the escape rates increase after a certain threshold in the available energy (Schillings et al., 2019), that the average energy of the ions decreases with an increase in the available energy (Lennartsson et al., 2004), and that the escape rates are dependent on the orientation of the IMF (Slapak et al., 2015). We look forward to future studies of the escaping energy at Earth and its coupling with the upstream solar wind, which can provide a more detailed comparison with its sibling planets Venus and Mars.

As the available energy in the solar wind was shown to have the largest influence on the escape rates from Venus, Venus was denoted as energy-limited in its escape (Persson et al., 2020a). This stands in contrast with the source-limited case for Mars, where the photoionization rate and supply of ions to the escaping source region are the factors that has the most influence on the escape rates (Ramstad et al., 2015). From this study, it is clear that even though the energy input to the system is important, the efficiency of this energy transfer becomes smaller as the available energy in the solar wind increases. From this one might argue that Venus is not purely energy-limited, as the increase in energy does not linearly scale the escape rates. However, it is clear that the more energy you put into the system, the more ions reach above the escape energy and can escape the planet, even though the energy input becomes less efficient the more energy is available. To understand the physics of this process in detail, the coupling needs to be further investigated during the extreme space weather events, when the dynamic pressure increases significantly. In addition, the coupling between the ionosphere and the neutral atmosphere needs to be quantified, as a part of the energy from the solar wind may be provided to the neutral atmosphere (Lundin et al., 2011), which would increase the efficiency of energy transferred from the solar wind to the Venusian atmosphere.

As the results indicate that the energy transfer from the solar wind to Venus is low (~0.01%), and decreases as the energy in the upstream solar wind increases, the historical energy transfer might also have been low. If the energy transfer from the solar wind to the ionosphere was low, the total effect on the Venusian atmospheric evolution might have been low. Therefore, we might speculate that some other process than the average long term ion escape have acted as the major loss process of water from Venus. For example, extreme space weather events, which mainly become averaged out in this large statistical study, may historically have had a larger effect on the escape rates, and the coupling between the solar wind and the Venusian ionosphere, than found in this study. Another explanation could be that the water was to a larger degree lost through interactions between the surface and the atmosphere, and/or water did not exist at a large extent on Venus after about 3.9 Gyrs ago.

4. Conclusions

Using measurements by the Ion Mass Analyzer, part of the ASPERA-4 instrument on board Venus Express, we have calculated the coupling between the upstream solar wind and the ion escape from Venus. On average about 0.01% of the energy available in the solar wind is transferred to the ions that escape from Venus. We have shown that the efficiency of energy transferred decreases with an increase in available energy in the solar wind. The results are similar to those found at Mars, where the coupling coefficient between the solar wind and the ion escape also decreases with an increase in the available upstream energy. However, the coupling at Mars is higher than at Venus by almost two orders of magnitude. On the contrary, the coupling behaves differently than at Earth, where the escape rate was found to only increase after a threshold was reached in the energy supplied to the system.

The results indicate that today the Venusian induced magnetosphere efficiently screens the atmosphere, limiting a solar wind driven atmospheric ion escape. The trend of decreased coupling with an increase in available energy upstream also indicates that the coupling might have been lower in the earlier history. Therefore, unless extreme space weather events had a significantly large effect on the escape rates in the

past 3.9 Gyrs, the water loss from Venus was presumably a consequence of another process than the long term escape rates induced by the interaction between the Venusian ionosphere and the solar wind.

Data Availability Statement

ASPERA-4/IMA data used in this study are publicly available via the ESA Planetary Science Archive (PSA; https://www.cosmos.esa.int/web/psa/venus-express). In addition, we acknowledge the use of Solar EUV Experiment (SEE) data from the Thermosphere Ionosphere Mesosphere Energetics Dynamics (TIMED) spacecraft and P.I. Thomas N. Woods. The data plotted in each figure presented here are available in the in-text data citation reference Persson et al. (2020b) and the identical mirror at https://data.irf.se/persson2020grl/.

Acknowledgments
The Swedish contribution to the ASPERA-4 experiment on board Venus Express was supported by the Swedish National Space Agency (SNSA). We acknowledge the European Space Agency (ESA) for supporting the successful Venus Express mission. M. Persson acknowledges support to her graduate studies from SNSA (Dnr: 129/14).

References

Barabash, S., Sauvaud, J.-A., Gunell, H., Andersson, H., Grigoriev, A., Brinkefeldt, K., et al. (2007). The analyzer of space plasmas and energetic atoms (ASPERA-4) for the Venus Express mission. *Planetary and Space Science*, *55*, 1772–1792.

Bergman, S., Stenberg Wieser, G., Wieser, M., Johansson, F., & Eriksson, A. (2020). The influence of spacecraft charging on low-energy ion measurements made by RPC-ICA on Rosetta.. *Journal of Geophysical Research: Space Physics*, *125*(1), e2019JA027478. https://doi.org/10.1029/2019JA027478

Bouhram, M., Klecker, B., Paschmann, G., Haaland, S., Hasegawa, H., Blagau, A., et al. (2005). Survey of energetic O^+ ions near the dayside mid-latitude magnetopause with Cluster. *Annales Geophysicae*, *23*, 1281–1294. https://doi.org/10.5194/angeo-23-1281-2005

Brace, L. H., Kasprzak, W. T., Taylor, H. A., Theis, R. F., Russell, C. T., Barnes, A., et al. (1987). The ionotail of Venus: Its configuration and evidence for ion escape. *Journal of Geophysical Research*, *92*(A1), 15–26.

Collinson, G. A., Frahm, R. A., Glocer, A., Coates, A. J., Grebowsky, J. M., Barabash, S., et al. (2016). The electric wind of Venus: A global and persistent "polar wind"-like ambipolar electric field sufficient for the direct escape of heavy ionospheric ions. *Geophysical Research Letters*, *43*(12), 5926–5934. https://doi.org/10.1002/2016GL068327

Cully, C. M., Donovan, E. F., Yau, A. W., & Opgenoorth, H. J. (2003). Supply of thermal ionospheric ions to the central plasma sheet. *Journal of Geophysical Research*, *108*(A2), 1092. https://doi.org/10.1029/2002JA009457

Dungey, J. W., (1961). Interplanetary magnetic field and the auroral zones. *Physical Review Letters*, *6*, 47–48. https://doi.org/10.1103/PhysRevLett.6.47

Edberg, N. J. T., Nilsson, H., Futaana, Y., Stenberg, G., Lester, M., Cowley, S. W. H., et al. (2011). Atmospheric erosion of Venus during stormy space weather. *Journal of Geophysical Research*, *116*(A9), A09308. https://doi.org/10.1029/2011JA016749

Fedorov, A., Barabash, S., Sauvaud, J.-A., Futaana, Y., Zhang, T. L., Lundin, R., & Ferrier, C. (2011). Measurements of the ion escape rates from Venus for solar minimum. *Journal of Geophysical Research*, *116*, A07220. https://doi.org/10.1029/2011JA016427

Futaana, Y., Stenberg Wieser, G., Barabash, S., & Luhmann, J. G. (2017). Solar wind interaction and impact on the Venus atmosphere. *Space Science Reviews*, *212*(3), 1453–1509.

Garrett, H. B. (1981). The charging of spacecraft surfaces. *Reviews of Geophysics*, *19*(4), 577–616. https://doi.org/10.1029/RG019i004p00577

Knudsen, W. C., Spenner, K., Miller, K. L., & Novak, V. (1980). Transport of ionospheric O+ ions across the Venus terminator and implications. *Journal of Geophysical Research*, *85*(A13), 7803–7810.

Kronberg, E. A., Ashour-Abdalla, M., Dandouras, I., Delcourt, D. C., Grigorenko, E. E., Kistler, L. M., et al. (2014). Circulation of heavy ions and their dynamical effects in the magnetosphere: Recent observations and models. *Space Science Reviews*, *184*, 173–235. https://doi.org/10.1007/s11214-014-0104-0

Lammer, H., Lichtenegger, H., Biernat, H., Erkaev, N., Arshukova, I., Kolb, C., et al. (2006). Loss of hydrogen and oxygen from the upper atmosphere of Venus. *Planetary and Space Science*, *54*(13–14), 1445–1456. https://doi.org/10.1016/j.pss.2006.04.022

Lennartsson, O. W., Collin, H. L., & Peterson, W. K. (2004). Solar wind control of Earth's H^+ and O^+ outflow rates in the 15-eV to 33-keV energy range. *Journal of Geophysical Research*, *109*, A12212. https://doi.org/10.1029/2004JA010690

Luhmann, J. G., Kasprzak, W. T., & Russell, C. T. (2007). Space weather at Venus and its potential consequences for atmosphere evolution. *Journal of Geophysical Research*, *112*(E4).E04S10. https://doi.org/10.1029/2006JE002820

Luhmann, J. G., Ledvina, S. A., & Russell, C. T. (2004). Induced magnetospheres. *Advances in Space Research*, *33*, 1905–1912.

Lundin, R., Barabash, S., Futaana, Y., Holmström, M., Sauvaud, J. A., & Fedorov, A. (2014). Solar wind-driven thermospheric winds over the Venus north polar region. *Geophysical Research Letters*, *41*, 4413–4419. https://doi.org/10.1002/2014GL060605

Lundin, R., Barabash, S., Futaana, Y., Sauvaud, J. A., Fedorov, A., & Perez-de-Tejada, H. (2011). Ion flow and momentum transfer in the Venus plasma environment. *Icarus*, *215*(2), 751–758. https://doi.org/10.1016/j.icarus.2011.06.034

Maggiolo, R., Sauvaud, J.-A., Fontaine, D., Teste, A., Grigorenko, E., Balogh, A., et al. (2006). A multi-satellite study of accelerated ion beams above the polar cap. *Annales Geophysicae*, *24*(6), 1665–1684. https://doi.org/10.5194/angeo-24-1665-2006

Marquette, M., Lillis, R. J., Halekas, J. S., Luhmann, J. G., Gruesbeck, J. R., & Espley, J. R. (2018). Autocorrelation study of solar wind plasma and IMF properties as measured by the MAVEN spacecraft. *Journal of Geophysical Research: Space Physics*, *123*, 2493–2512. https://doi.org/10.1002/2018JA025209

Martinecz, C., Fränz, M., Woch, J., Krupp, N., Roussos, E., Dubinin, E., et al. (2008). Location of the bow shock and ion composition boundary at Venus—Initial determinations from Venus Express ASPERA-4. *Planetary and Space Science*, *56*(6), 780–784. https://doi.org/10.1016/j.pss.2007.07.007

Masunaga, K., Futaana, Y., Persson, M., Barabash, S., Zhang, T., Rong, Z. J., et al. (2019). Effects of the solar wind and the solar EUV flux on O+ escape rates from Venus. *Icarus*, *321*, 379–387. https://doi.org/10.1016/j.icarus.2018.11.017

McComas, D. J., Spence, H. E., Russell, C. T., & Saunders, M. A. (1986). The average magnetic field draping and consistent plasma properties of the Venus magnetotail. *Journal of Geophysical Research*, *91*(A7), 7939–7953.

McEnulty, T. R.. (2012). *Oxygen loss from Venus and the influence of extreme solar wind conditions*. ProQuest Dissertations And Theses, Doctoral dissertation. UC Berkeley Library, CA. http://digitalassets.lib.berkeley.edu/etd/ucb/text/McEnulty_berkeley_0028E_13126.pdf

Moore, T., Fok, M.-C., & Garcia-Sage, K. (2014). The ionospheric outflow feedback loop. *Journal of Atmospheric and Solar-Terrestrial Physics*, *115–116*, 59–66. https://doi.org/10.1016/j.jastp.2014.02.002

Nilsson, H., Barghouthi, I. A., Slapak, R., Eriksson, A. I., & Andŕe, M. (2012). Hot and cold ion outflow: Spatial distribution of ion heating. *Journal of Geophysical Research*, *117*, A11201. https://doi.org/10.1029/2012JA017974

Nilsson, H., Barghouthi, I. A., Slapak, R., Eriksson, A. I., & Andŕe, M. (2013). Hot and cold ion outflow: Observations and implications for numerical models. *Journal of Geophysical Research*, *118*, 105–117. https://doi.org/10.1029/2012JA017975

Nilsson, H., Waara, M., Marghitu, O., Yamauchi, M., Lundin, R., R`eme, H., et al. (2008). An assessment of the role of the centrifugal acceleration mechanism in high altitude polar cap oxygen ion outflow. *Annales Geophysicae*, *26*, 145–157. https://doi.org/10.5194/angeo-26-145-2008

Pérez-De-Tejada, H. (1980), Evidence for a viscous boundary layer at the Venus ionopause from the preliminary Pioneer Venus results. *Journal of Geophysical Research*, *85*(A13), 7709–7714. https://doi.org/10.1029/JA085iA13p07709

Persson, M., Futaana, Y., Fedorov, A., Nilsson, H., Hamrin, M., & Barabash, S. (2018). H+/O+ escape rate ratio in the Venus magnetotail and its dependence on the solar cycle. *Geophysical Research Letters*, *45*(20), 10805–10811. https://doi.org/10.1029/2018GL079454

Persson, M., Futaana, Y., Ramstad, R., Masunaga, K., Nilsson, H., Hamrin, M., et al. (2020a). The Venusian atmospheric oxygen ion escape: Extrapolation to the Early Solar System. *Journal of Geophysical Research: Planets*, *125*, e2019JE006336. https://doi.org/10.1029/2019JE006336

Persson, M., Futaana, Y., Nilsson, H., Stenberg Wieser, G., Hamrin, M., Fedorov, A., et al. (2019). Heavy ion flows in the upper ionosphere of the Venusian north pole. *Journal of Geophysical Research: Space Physics*, *124*(6), 4597–4607.

Persson, M., Futaana, Y., Ramstad, R., Schillings, A., Masunaga, K., Nilsson, H., et al. (2020b). *Supplementary data for: "Global Venus-solar Wind coupling and oxygen ion escape"*. Dataset Zeonodo. https://doi.org/10.5281/zenodo.4327220

Ramstad, R., Barabash, S., Futaana, Y., Nilsson, H., & Holmström, M. (2017). Global mars-solar wind coupling and ion escape. *Journal of Geophysical Research: Space Physics*, *122*(8), 8051–8062. https://doi.org/10.1002/2017JA024306

Ramstad, R., Barabash, S., Futaana, Y., Nilsson, H., & Holmström, M. (2018). Ion escape from mars through time: An extrapolation of atmospheric loss based on 10 years of mars express measurements. *Journal of Geophysical Research: Planets*, *123*(11), 3051–3060. https://doi.org/10.1029/2018JE005727

Ramstad, R., Barabash, S., Futaana, Y., Nilsson, H., Wang, X.-D., & Holmström, M. (2015). The Martian atmospheric ion escape rate dependence on solar wind and solar EUV conditions: 1. seven years of Mars Express observations. *Journal of Geophysical Research: Planets*, *120*, 1298–1309. https://doi.org/10.1002/2015JE004816

Ribas, I., Guinan, E. F., Gu¨del, M., & Audard, M. (2005). Evolution of the solar activity over time and effects on planetary atmospheres. I. high-energy irradiances (1–1700Å). *The Astrophysical Journal*, *622*(1), 680.

Russell, C. T., Chou, E., Luhmann, J. G., & Brace, L. H. (1990). Solar cycle variations in the neutral exosphere inferred from the location of the Venus bow shock. *Advances in Space Research*, *10*(5), 5–9. https://doi.org/10.1016/0273-1177(90)90159-W

Schillings, A., Gunell, H., Nilsson, H., De Spiegeleer, A., Ebihara, Y., Westerberg, L. G., et al. (2020). The fate of O^+ ions observed in the plasma mantle: particle tracing modeling and cluster observations. *Annales Geophysicae*, *38*(3), 645–656. https://doi.org/10.5194/angeo-38-645-2020

Schillings, A., Slapak, R., Nilsson, H., Yamauchi, M., Dandouras, I., & Westerberg, L.-G. (2019). Earth atmospheric loss through the plasma mantle and its dependence on solar wind parameters. *Earth, Planets and Space*, *71*(1), 70.

Slapak, R., Nilsson, H., Waara, M., Andŕe, M., Stenberg, G., & Barghouthi, I. A. (2011). O^+ heating associated with strong wave activity in the high altitude cusp and mantle. *Annales Geophysicae*, *29*, 931–944. https://doi.org/10.5194/angeo-29-931-2011

Slapak, R., Nilsson, H., Westerberg, L. G., & Larsson, R. (2015). O^+ transport in the dayside magnetosheath and its dependence on the IMF direction. *Annales Geophysicae*, *33*, 301–307. https://doi.org/10.5194/angeo-33-301-2015

Slavin, J. A., Elphic, R. C., Russell, C. T., Scarf, F. L., Wolfe, J. H., Mihalov, J. D., et al. (1980). The solar wind interaction with Venus: Pioneer Venus observations of bow shock location and structure. *Journal of Geophysical Research*, *85*(A13), 7625–7641. https://doi.org/10.1029/JA085iA13p07625

Strangeway, R. J., Ergun, R. E., Su, Y.-J., Carlson, C. W., & Elphic, R. C. (2005). Factors controlling ionospheric outflows as observed at intermediate altitudes. *Journal of Geophysical Research*, *110*(A3), A03221. https://doi.org/10.1029/2004JA010829

Svedhem, H., Titov, D.V., McCoy, D., Lebreton, J.-P., Barabash, S., Bertaux, J.-L., et al. (2007). Venus Express - The first European mission to Venus. *Planetary and Space Science*, *55*(12), 1636–1652. https://doi.org/10.1016/j.pss.2007.01.013

Thiemann, E. M. B., Eparvier, F. G., & Woods, T. N. (2017). A time dependent relation between EUV solar flare light-curves from lines with differing formation temperatures. *Journal of Space Weather and Space Climate*, *7*(A36), 12.

Way, M. J., Del Genio, A. D., Kiang, N. Y., Sohl, L. E., Grinspoon, D. H., Aleinov, I., et al. (2016). Was Venus the first habitable world of our solar system? *Geophysical Research Letters*, *43*(16), 8376–8383. https://doi.org/10.1002/2016GL069790

Webb, D. F., & Howard, R. A. (1994). The solar cycle variation of coronal mass ejections and the solar wind mass flux. *Journal of Geophysical Research*, *99*(A3), 4201–4220. https://doi.org/10.1029/93JA02742

Wood, B. E. (2006). The solar wind and the sun in the past. *Space Science Reviews*, *126*(1), 3–14.

Woods, T. N., Eparvier, F. G., Bailey, S. M., Chamberlin, P. C., Lean, J., Rottman, G. J., et al. (2005). Solar EUV Experiment (SEE): Mission overview and first results. *Journal of Geophysical Research*, *110*, A01312. https://doi.org/10.1029/2004JA010765